Electronic Supplementary Material (ESI) for New Journal of Chemistry.
This journal is © The Royal Society of Chemistry and the Centre National de la Recherche Scientifique 2020

Electronic Supplementary Material

Studies of the stability, nucleophilic substitution reactions, DNA/BSA interactions, cytotoxic activity, DFT and molecular docking of some tetra- and penta-coordinated gold(III) complexes

Snežana Radisavljević,[a]Ana ĐekovićKesić,[b]Dušan Ćoćić,[a]Ralph Puchta,[c,d,e]
Laura Senft,[c]Milena Milutinović,[f]Nevena Milojević[f] and Biljana Petrović[1]*

DNA-binding studies

Calculation of binding constant toDNA

In order to compare the binding strength of the complexes, the intrinsic binding constants $K_b$were calculated according to the changes in absorption at the MLCT band with increasing concentration of DNA.The binding constant of the complexes with DNA(in M^{-1}), may be calculated by the ratio of the slope to the y intercept in plots $\frac{[DNA]}{(\varepsilon_A - \varepsilon_f)}$ *vs.* [DNA] (Inset in Figure 2), using the following equation(S1):[s1]

$$\frac{[DNA]}{(\varepsilon_A - \varepsilon_f)} = \frac{[DNA]}{(\varepsilon_b - \varepsilon_f)} + \frac{1}{K_b(\varepsilon_b - \varepsilon_f)} \qquad \text{(eq. S1)}$$

where [DNA] is the concentration of DNA in base pairs, ε_f is the extinction coefficient for the unbound complex at the corresponding λ_{max}, $\varepsilon_A = A_{obsd}/[complex]$ and ε_b is the extinction coefficient for the complex in the fully bound form.

Stern-Volmer equation for EB competitive studies

The Stern-Volmer plots of DNA-EB illustrate that the quenching of EB bound to DNA by the compounds is in good agreement (R = 0.95)with the linear Stern-Volmer equation:

$$\frac{Io}{I} = 1 + K_{SV}[Q] \qquad \text{(eq. S2)}$$

where I and I_0 are the emission intensities in the presence and absence of gold(III) complexes, [Q] is the final concentration of the quencher, K_{sv} is the Stern-Volmer quenching constant.

Stern-Volmer equation for BSA studies

The values of the dynamic quenching constant (K_{SV}, M^{-1}) and the quenching rate constant (k_q, M^{-1} s^{-1}) for the interaction of gold(III) complexes with BSA, were calculated using the Stern-Volmer quenching equation:

$$\frac{Io}{I} = 1 + k_q \tau_0 [Q] = 1 + K_{SV}[Q] \qquad \text{(eq. S3)}$$

where Io = the initial tryptophan fluorescence intensity of BSA, I = the tryptophan fluorescence intensity of BSA after the addition of complexes, k_q = the quenching rate constants of BSA, K_{SV} = the dynamic quenching constant, τ_o = the average lifetime of BSA without complexes, [Q] = the concentration of gold(III) complexes, $K_{SV} = k_q \tau_o$ and, taking as fluorescence lifetime (τ_o) of tryptophan in BSA at around 10^{-8} s.

Scatchard equation

Association binding constant (*K*) and number of binding sites per albumin (*n*) can be calculated using Scatchard equation, Eq. (S4)[s2]:

$$\frac{\Delta I}{I_0} \div [Q] = nK - K\frac{\Delta I}{I_0} \qquad \text{(eq. S4)}$$

where *K* may be calculated from the slope in the Scatchard plots $\frac{\Delta I}{I_0} \div [Q]$ *vs.* $\frac{\Delta I}{I_0}$ and *n* is given by the ratio of *y* intercept to the slope.

References

S1. S. Yu-Min, W. Qiong, Y. Pei-Ju, L. Ni-Na, W. Liu-Fang andL. Ying-Mei, *J. Inorg.Biochem.*, 2006,**100**, 1685-1691.

S2. S. S. Wu, W. B. Yuan, H. Y. Wang, Q. Zhang, M. Liu and K. B. Yu, *J Inorg. Biochem.*,2008, **102**, 2026-2034.

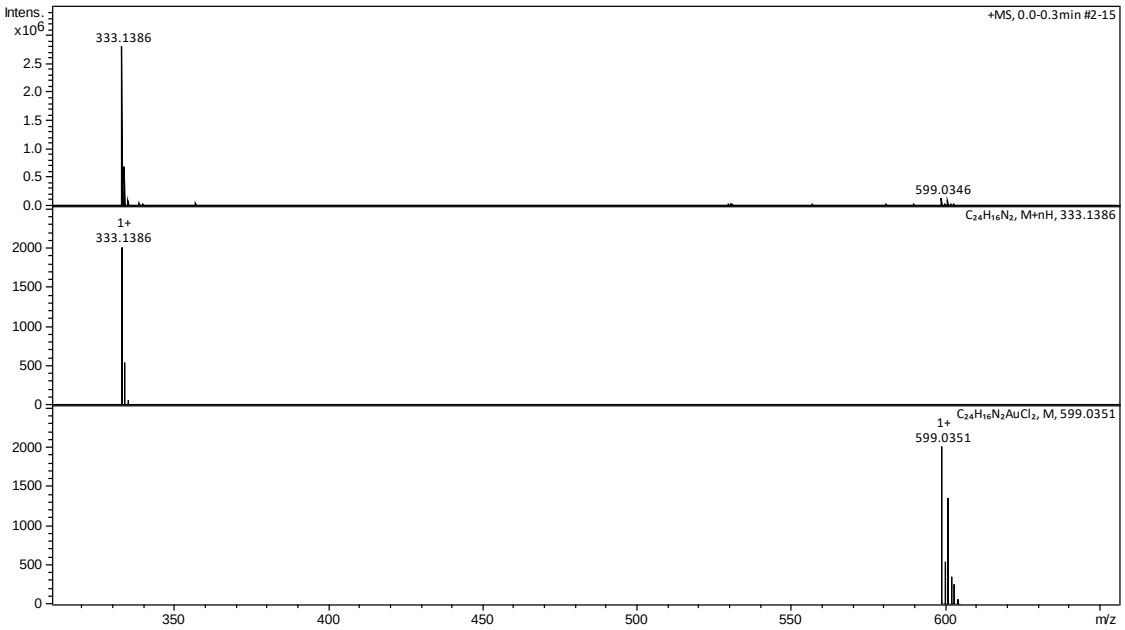

Figure S1. ESI-MS spectrum of complex **1**

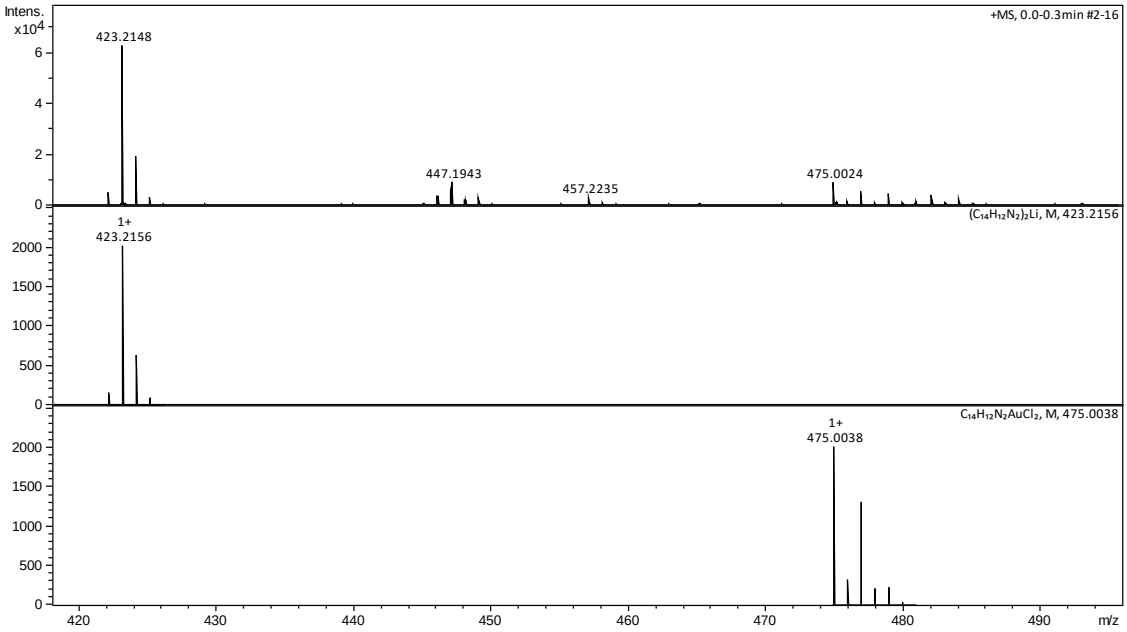

Figure S2. ESI-MS spectrum of complex **2**

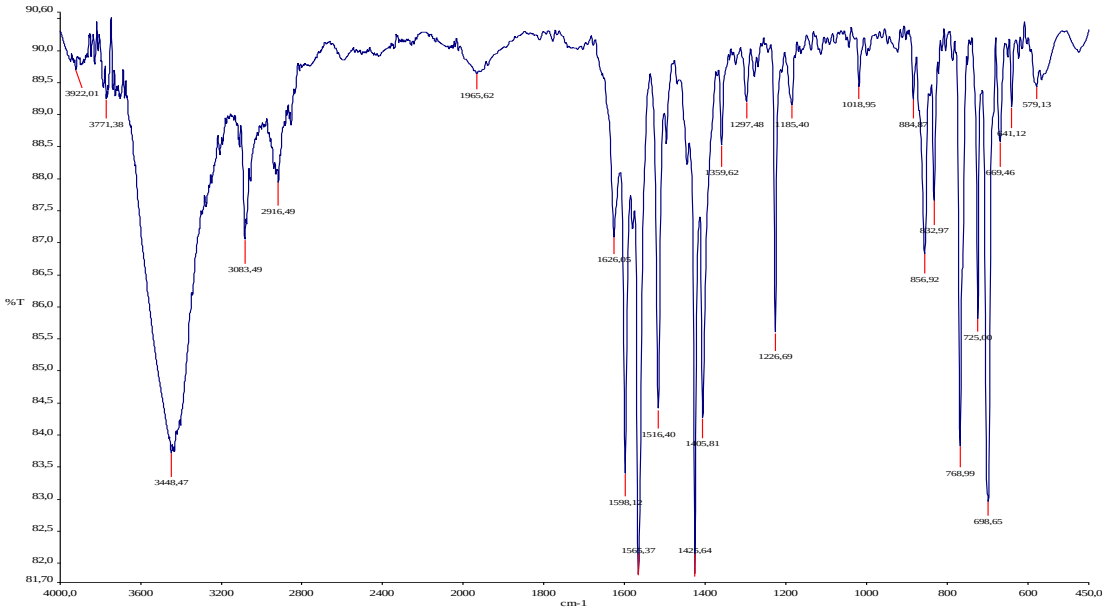

Figure S3. IR spectrum of complex **1**

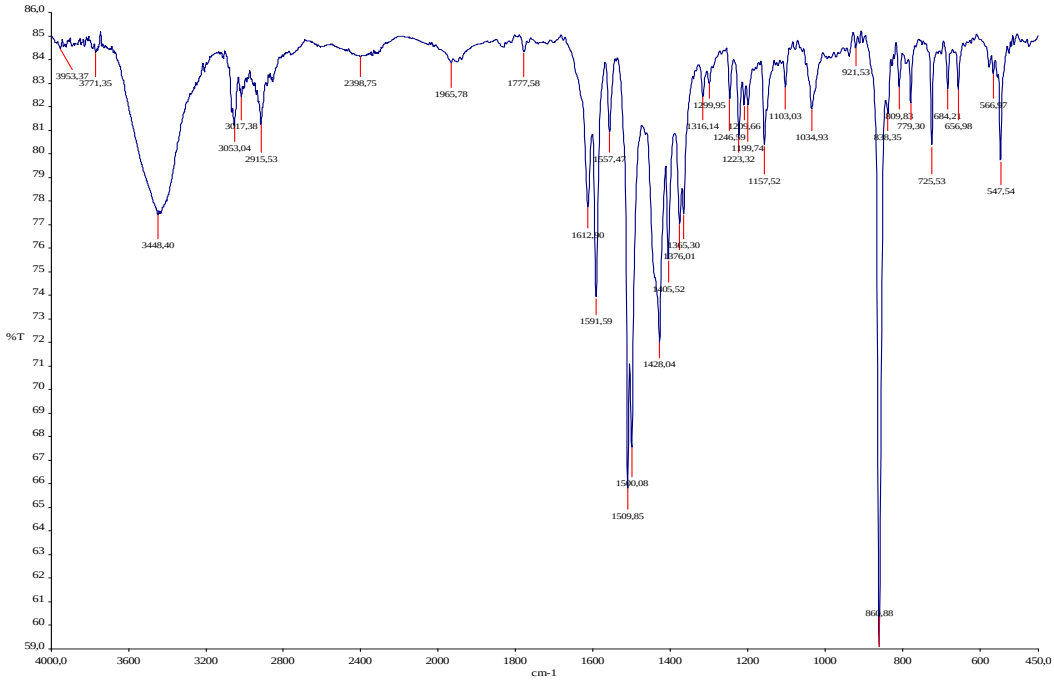

Figure S4. IR spectrum of complex **2**

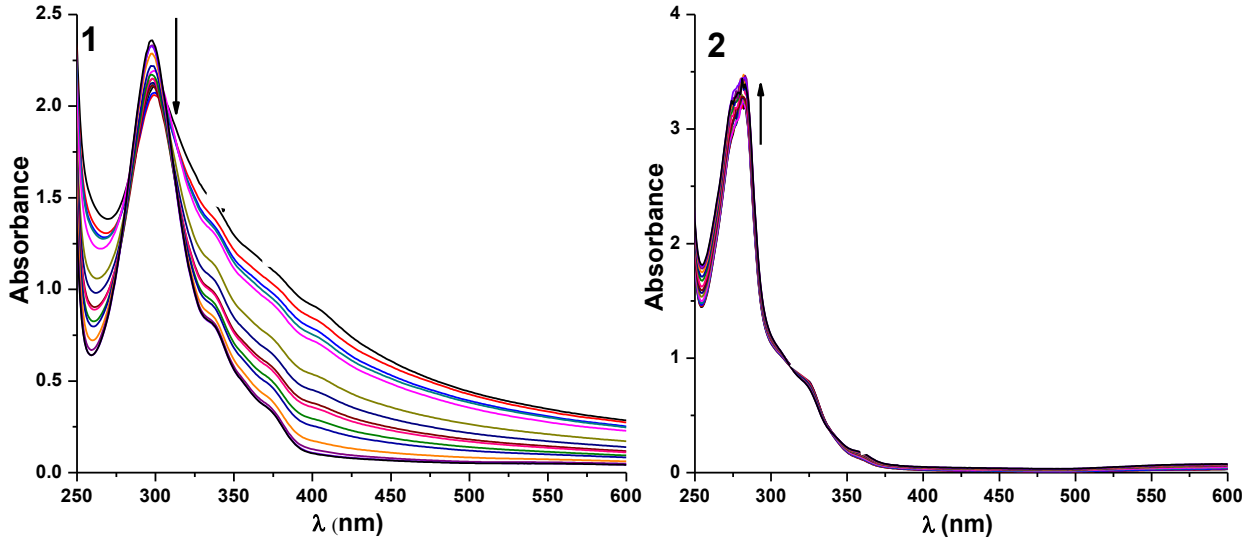

Figure S5. UV-Vis spectra of complexes **1**and **2** in water over a 6hours period.

[complex] = 1×10^{-4} M

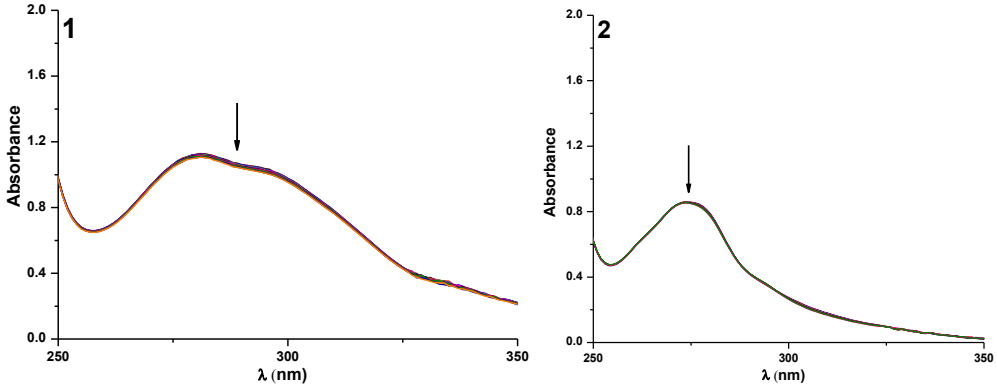

Figure S6. UV-Vis spectra of complexes **1** and **2** in Hepes buffer (pH=7.2) over a 6 hours period. [complex] = 5×10^{-5}M

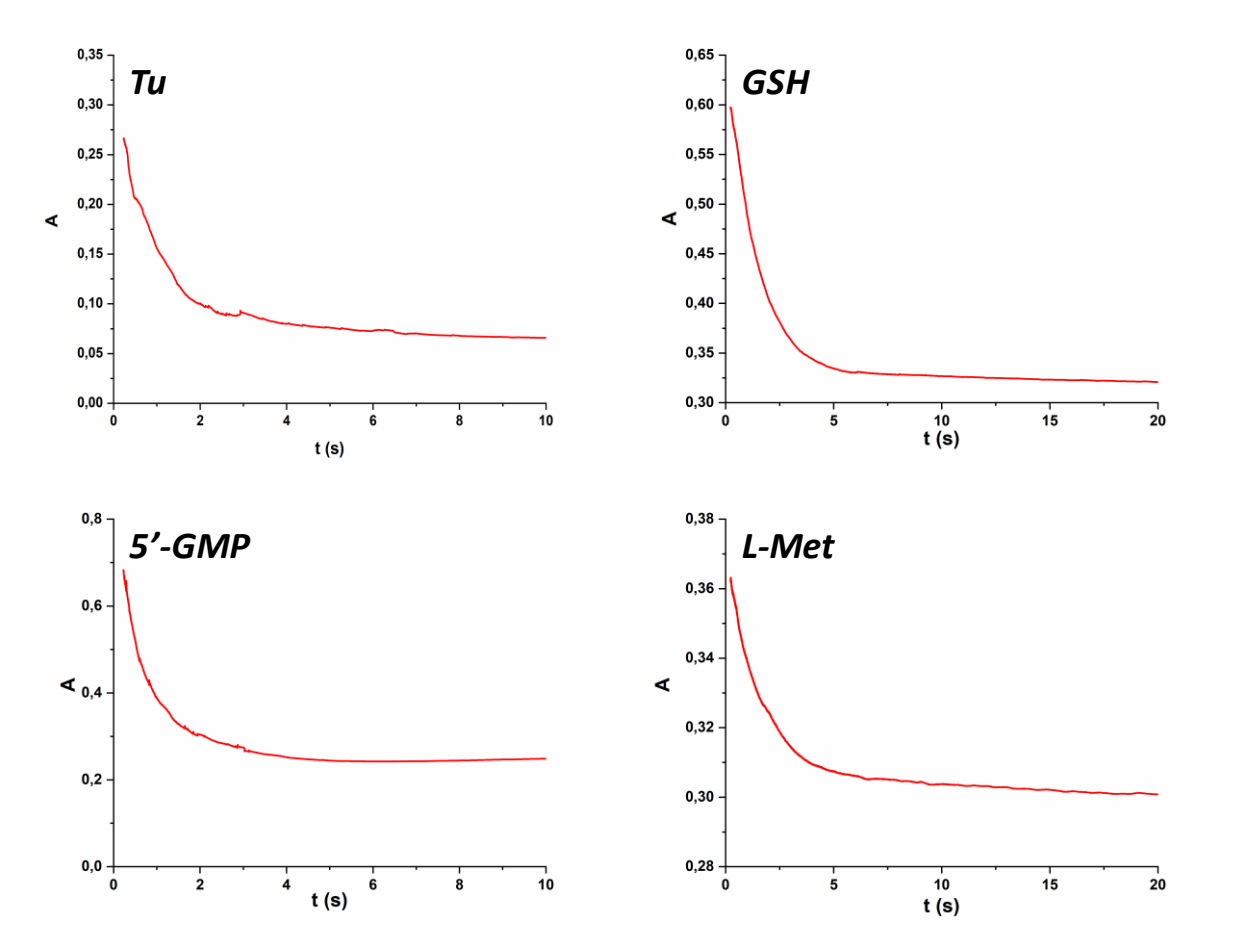

Figure S7. Kinetic traces for the substitution reactions of complex **1** with selected nucleophiles

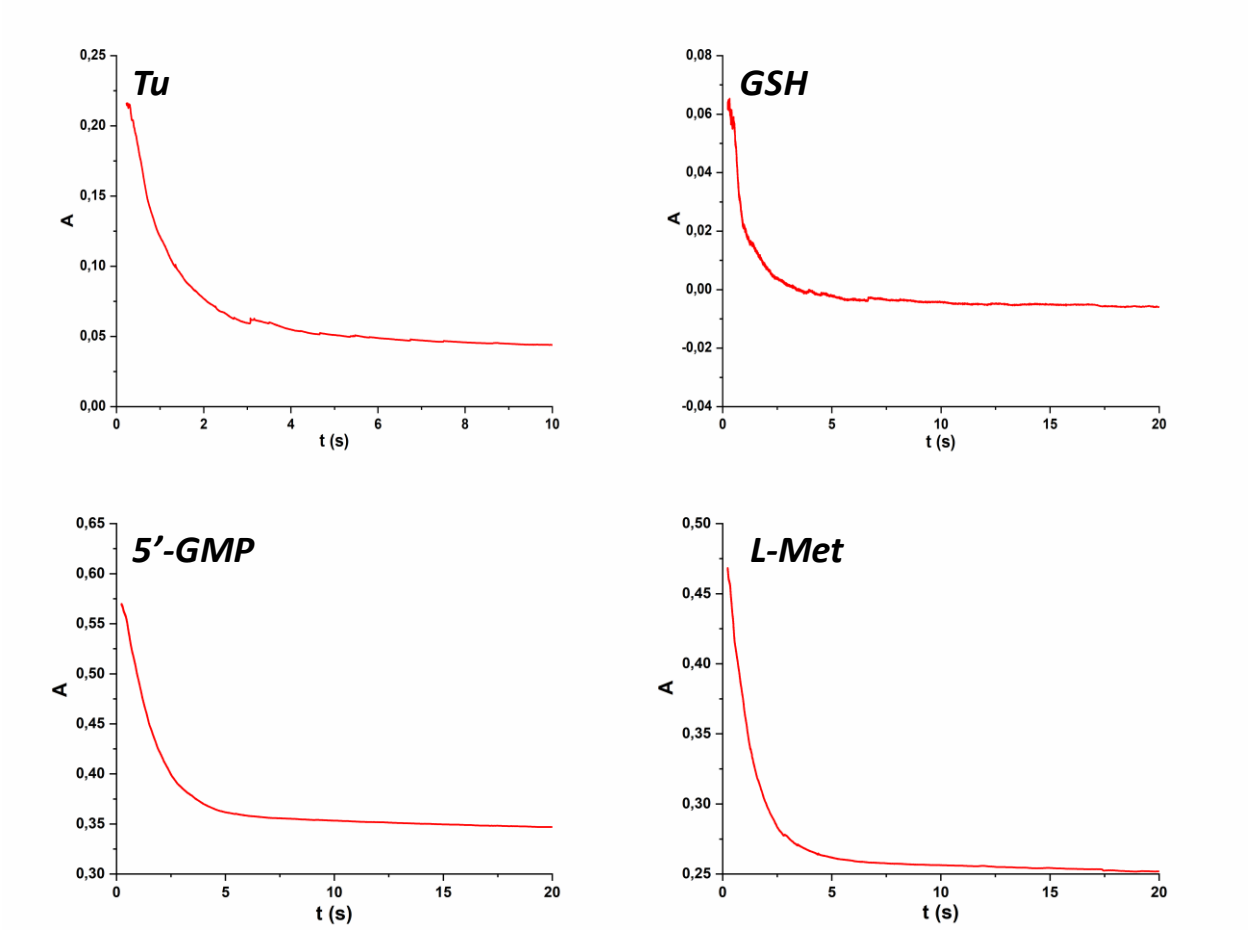

Figure S8. Kinetic traces for the substitution reactions of complex **2** with selected nucleophiles

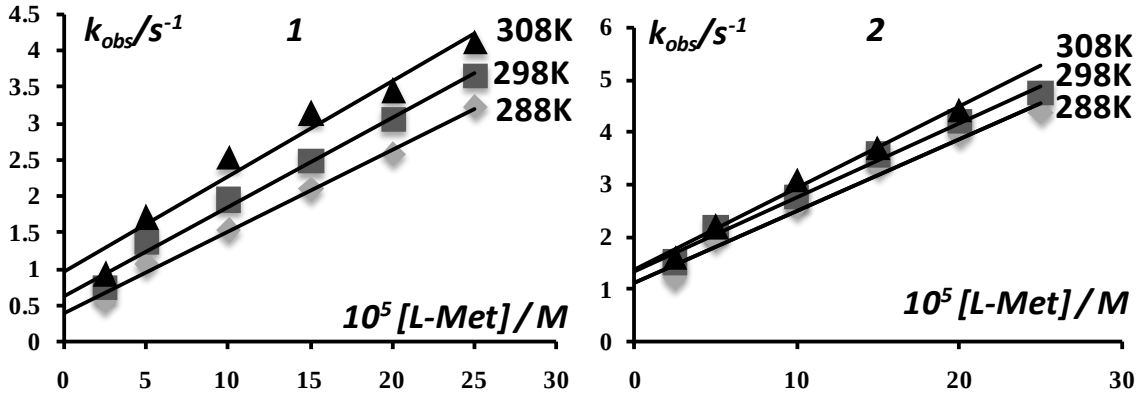

Figure S9. Pseudo-first order rate constants for the substitution reactions between complexes **1** and **2** with L-Met, as a function of nucleophile concentration and temperature, at pH = 7.2 (25 mM Hepes buffer) with the addition of 30 mM NaCl.

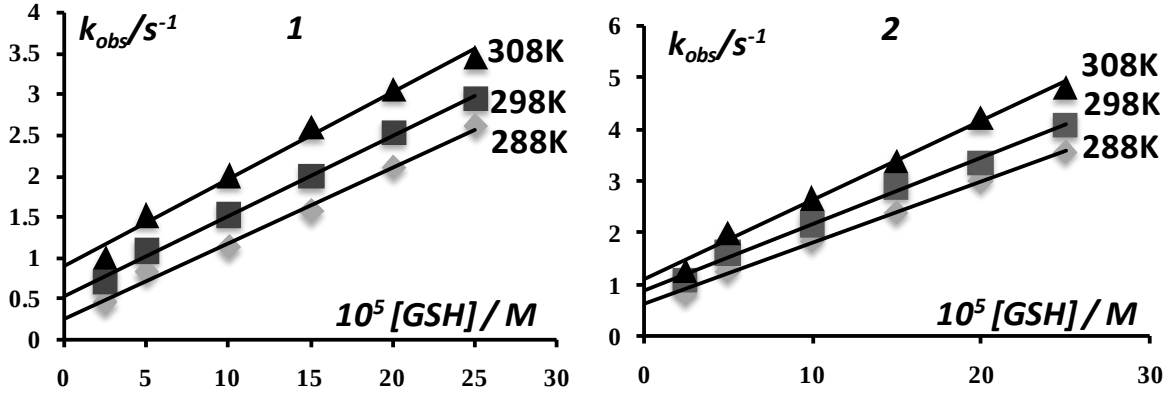

Figure S10. Pseudo-first order rate constants for the substitution reactions between complexes **1** and **2** with GSH, as a function of nucleophile concentration and temperature, at pH = 7.2 (25 mM Hepes buffer) with the addition of 30 mM NaCl.

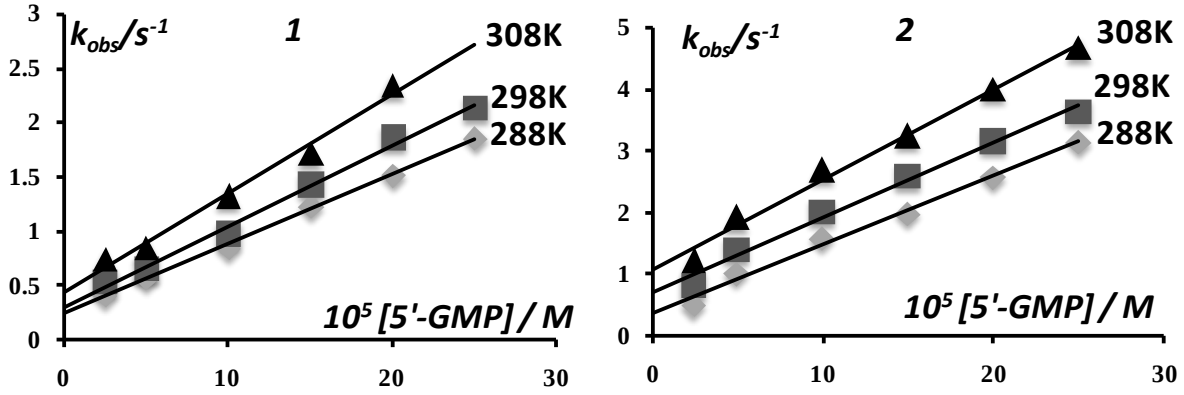

Figure S11. Pseudo-first order rate constants for the substitution reactions between complexes **1** and **2** with 5'-GMP, as a function of nucleophile concentration and temperature, at pH = 7.2 (25 mM Hepes buffer) with the addition of 30 mM NaCl.

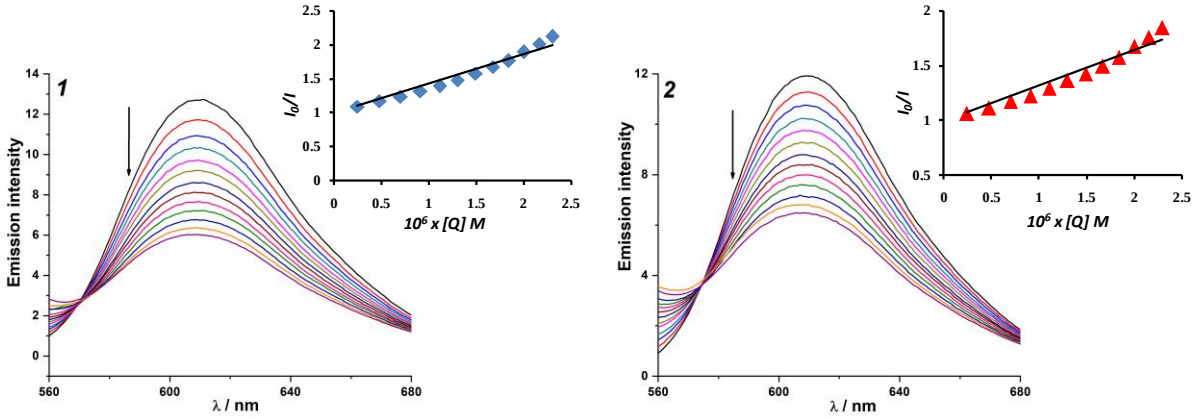

Figure S12. Fluorescence emission spectra (λ_{ex}= 527 nm) of the EB-DNA system (5×10^{-6} M EB, 5×10^{-6} M DNA) in the absence and in the presence of complexes **1** and **2** (1×10^{-4} M, 62.5μL per scan). Arrows show the intensity changes upon increasing the concentration of complex. Insert: Stern-Volmer quenching plot of DNA-EB.

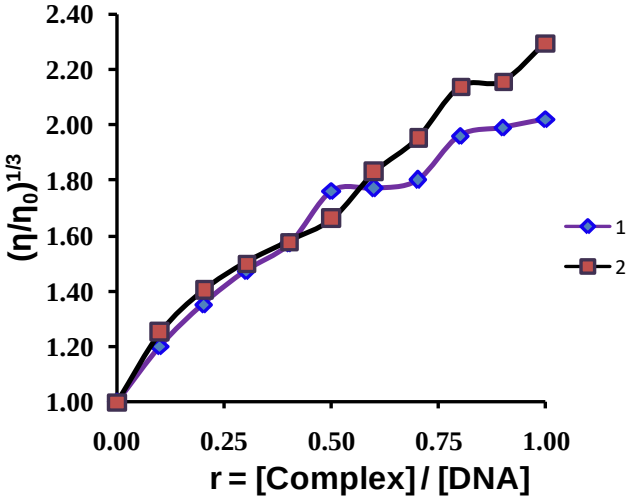

Figure S13. Relative viscosity $(\eta/\eta_o)^{1/3}$ of CT-DNA (11 μM) in buffer solution (25 mM Hepes, 30mM NaCl) in the presence of increasing amounts of complexes **1** and **2** (r).

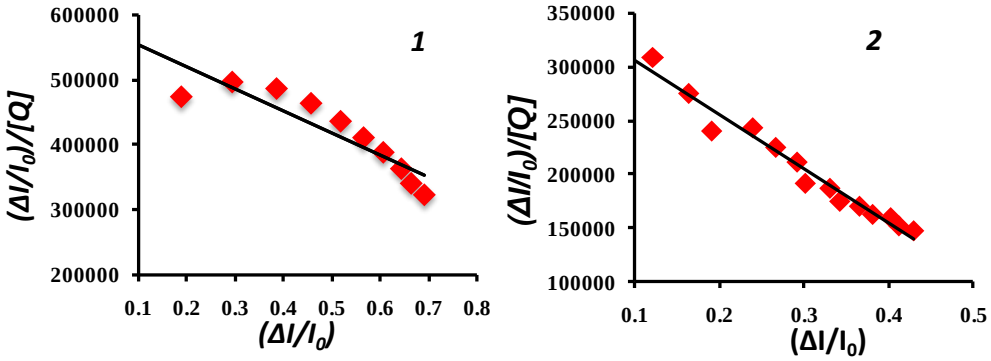

Figure S14. Scatchard plots for complexes **1** and **2.**

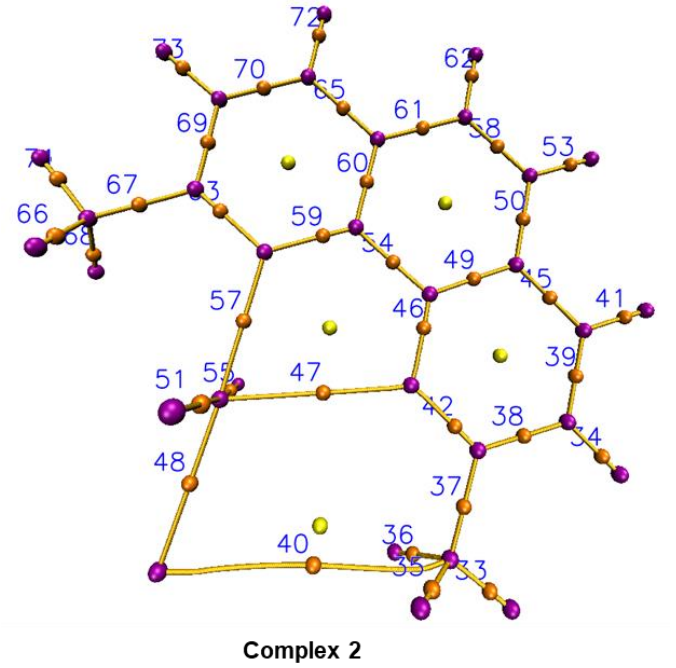

Figure S15. AIM plot of complex **2** with labels for bond critical points (BCP).

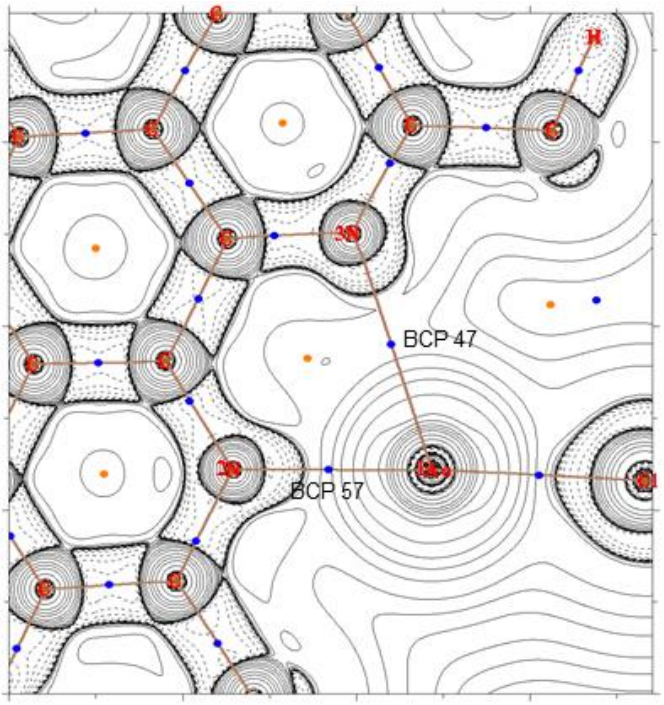

Figure S16. Laplacian of electron density presented in contour line map along 2N-1Au-3N plane (BCPs are presented as blue dots while bond paths are presented as brow lines).

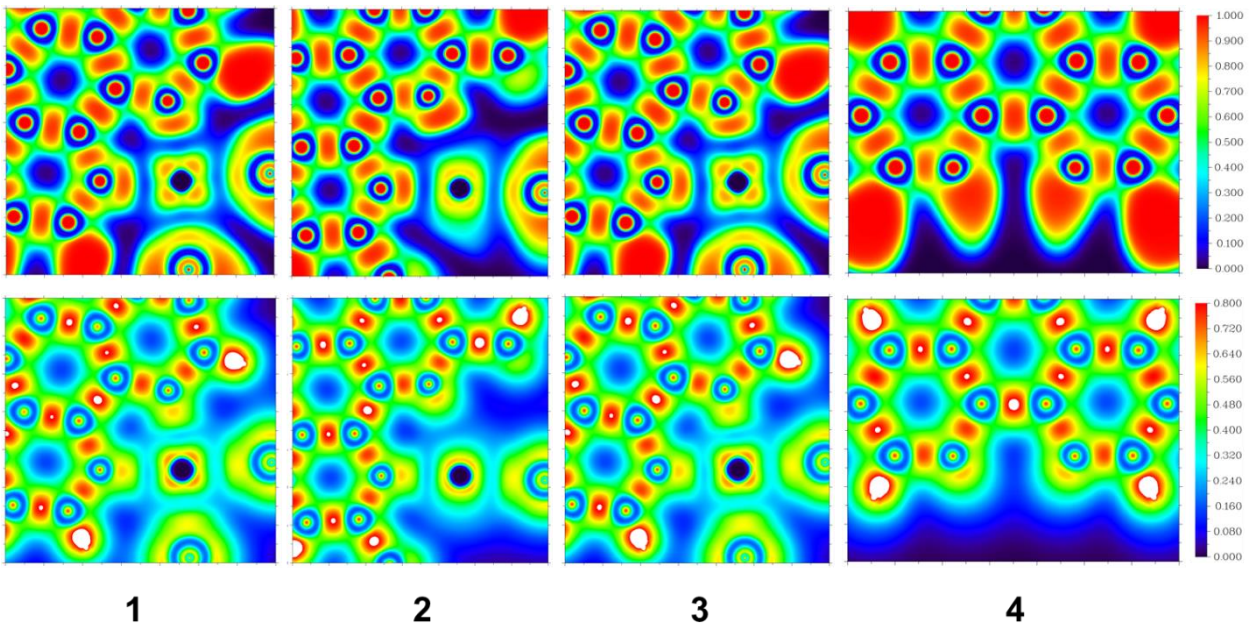

Figure S17. The electron localization function (ELF) (upper) and localized orbital locator (LOL) (lower) of **1, 2, 3** and **4** presented in color filed map along N-Au-N plane.

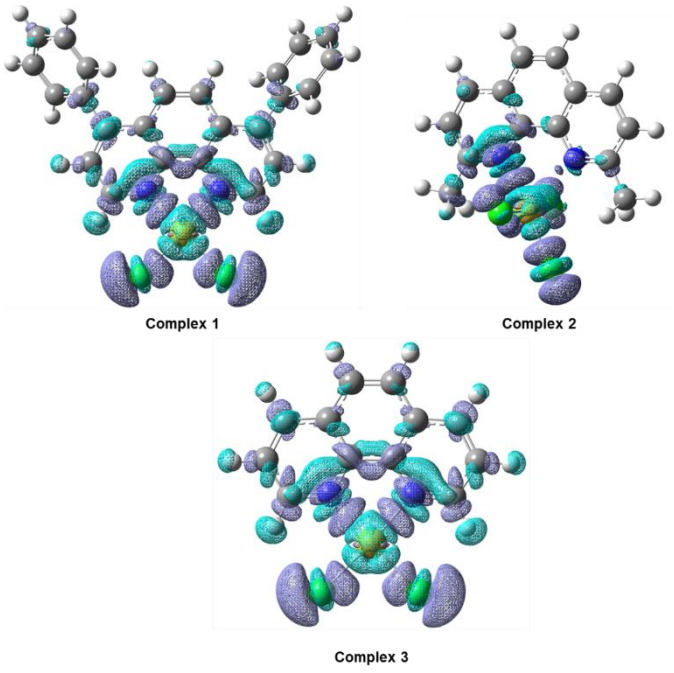

Figure S18. Grid data of electron density difference for complexes **1**, **2** and **3** (isoval = 0.003).

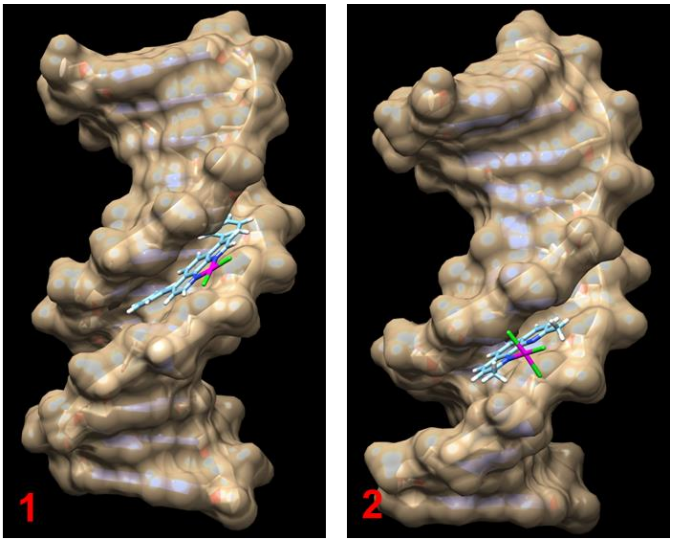

Figure S19. Computational docking model illustrating interactions between investigated complexes and canonical B-DNA.

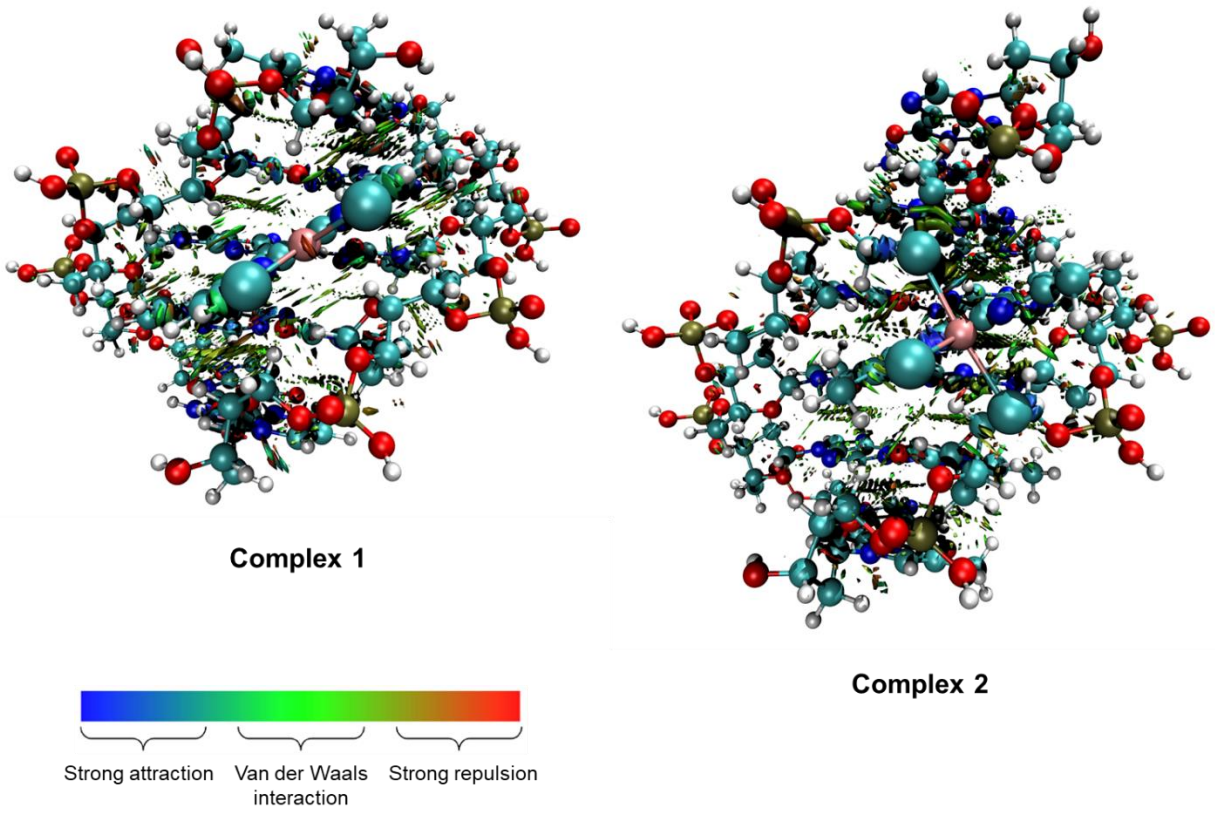

Figure S20. NCI plot for a representative conformation of complexes **1** and **2** docked in the canonical B-DNA, surfaces represent the non-covalent interactions according to the color bar (isoval = 0.3).

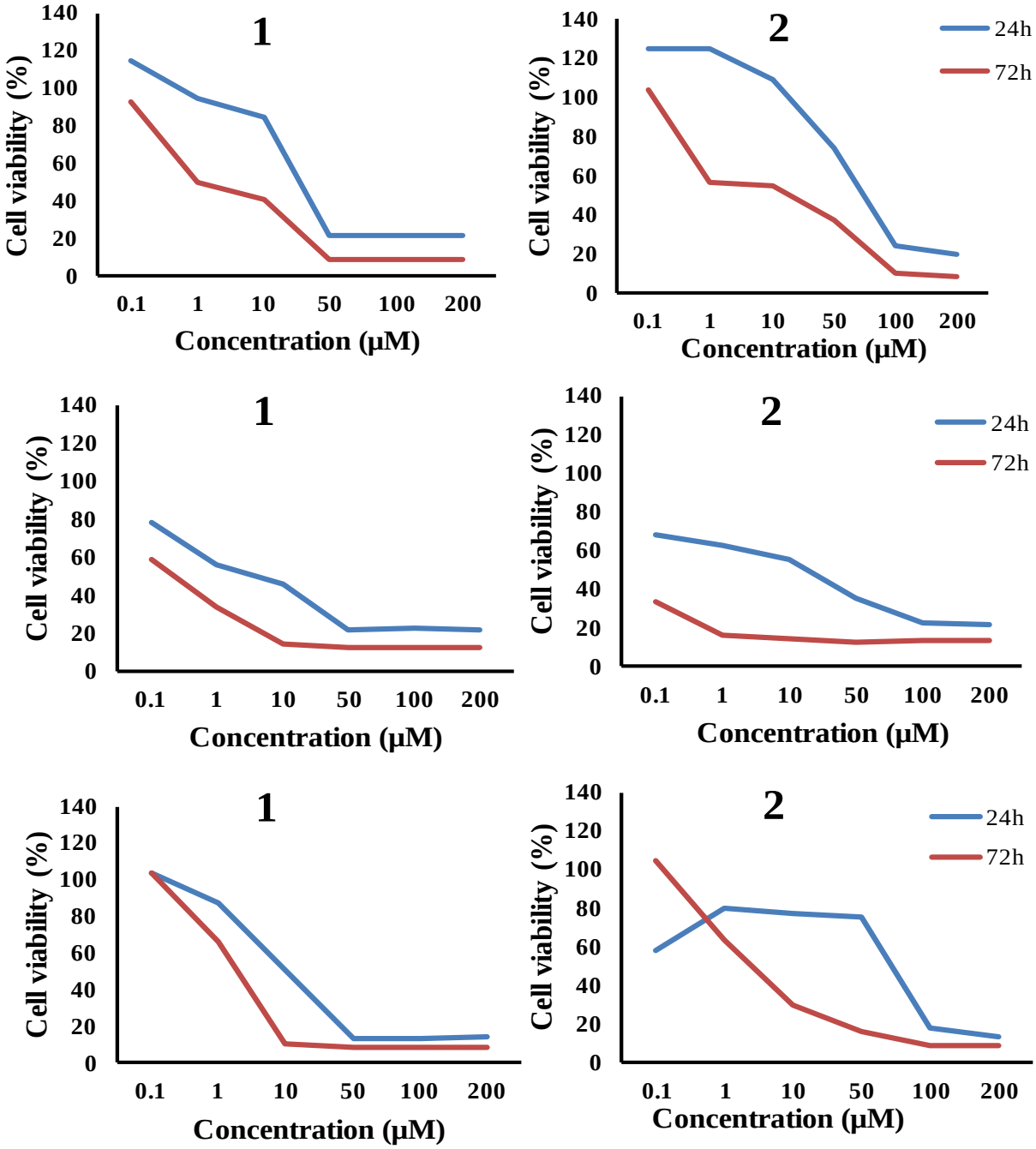

Figure S21. The effect of complexes **1** and **2** on the MDA-231 (top); HCT-116 (middle) and HaCaT (bottom) cell viability after 24 and 72 h of exposure. All values are mean, n=6; percentages of viable cells.

Table S1. Observed *pseudo*-first order rate constants (for the first and the second reaction steps) as a function of ligand concentration and temperature for the substitution reactions between complex **1** and Tu in 25 mM Hepes buffer and 30 mM NaCl (pH=7.2).

λ/nm	T/K	$10^{-4}C_L$/M	k_{obs1}/s^{-1}	k_{obs2}/s^{-1}
276	288	0.25	6.165(6)[a]	1.360(6)[a]
		0.5	7.595(5)	1.960(5)
		1	8.920(6)	2.450(6)
		1.5	10.230(6)	2.770(6)
		2	11.610(5)	3.565(5)
		2.5	12.580(6)	4.083(6)
	298	0.25	7.333(5)	2.070(5)
		0.5	8.770(5)	2.855(5)
		1	10.100(6)	3.443(6)
		1.5	11.615(5)	4.160(5)
		2	13.057(5)	5.040(5)
		2.5	14.728(6)	6.145(6)
	308	0.25	8.465(6)	2.690(6)
		0.5	10.420(6)	3.030(6)
		1	12.010(6)	3.890(6)
		1.5	13.680(5)	4.910(5)
		2	15.480(5)	5.900(5)
		2.5	16.990(6)	6.640(6)

[a]Number of runs in parenthesis.

Table S2. Observed *pseudo*-first order rate constants as a function of ligand concentration and temperature for the substitution reactions between complex **1** and 5'-GMP in 25 mM Hepes buffer and 30 mM NaCl (pH=7.2).

λ/nm	T/K	$10^{-4}C_L$/M	k_{obs}/s^{-1}
255	288	0.25	0.407(5)[a]
		0.5	0.566(5)
		1	0.844(5)
		1.5	1.225(6)
		2	1.512(5)
		2.5	1.855(6)
	298	0.25	0.531(5)
		0.5	0.649(5)
		1	0.973(6)
		1.5	1.427(6)
		2	1.860(5)
		2.5	2.131(6)
	308	0.25	0.735(5)
		0.5	0.845(6)
		1	1.321(6)
		1.5	1.710(5)
		2	2.340(6)

Table S3. Observed *pseudo*-first order rate constants as a function of ligand concentration and temperature for the substitution reactions between complex **1** and GSH in 25 mM Hepes buffer and 30 mM NaCl (pH=7.2).

λ/nm	T/K	$10^{-4}C_L$/M	k_{obs}/s^{-1}
280	288	0.25	0.455(5)
		0.5	0.820(6)
		1	1.128(5)
		1.5	1.566(6)
		2	2.100(5)
		2.5	2.608(6)
	298	0.25	0.700(6)
		0.5	1.087(5)
		1	1.527(6)
		1.5	1.997(5)
		2	2.532(5)
		2.5	2.943(6)
	308	0.25	0.997(5)
		0.5	1.527(5)
		1	2.009(6)
		1.5	2.600(5)
		2	3.068(6)
		2.5	3.450(5)

Table S4. Observed *pseudo*-first order rate constants as a function of ligand concentration and temperature for the substitution reactions between complex **1** and L-Met in 25 mM Hepes buffer and 30 mM NaCl (pH=7.2)

λ/nm	T/K	$10^{-4}C_L$/M	k_{obs}/s^{-1}
295	288	0.25	0.560(6)
		0.5	1.056(6)
		1	1.524(5)
		1.5	2.082(5)
		2	2.571(5)
		2.5	3.220(6)
	298	0.25	0.738(5)
		0.5	1.360(6)
		1	1.945(5)
		1.5	2.470(6)
		2	3.050(5)
		2.5	3.643(5)
	308	0.25	0.930(5)
		0.5	1.710(6)
		1	2.530(5)
		1.5	3.145(5)
		2	3.455(6)
		2.5	4.113(5)

Table S5. Observed *pseudo*-first order rate constants (for the first and the second reaction steps) as a function of ligand concentration and temperature for the substitution reactions between complex **2** and Tu in 25 mM Hepes buffer and 30 mM NaCl (pH=7.2).

λ/nm	T/K	$10^{-4}C_L$/M	k_{obs1}/s^{-1}	k_{obs2}/s^{-1}
272	288	0.25	8.715(5)[a]	2.520(5)
		0.5	9.320(5)	2.810(5)
		1	10.837(6)	3.437(6)
		1.5	12.370(5)	4.138(5)
		2	13.776(6)	4.910(6)
		2.5	15.417(5)	5.347(5)
	298	0.25	9.940(6)	3.493(6)
		0.5	11.495(6)	4.400(6)
		1	13.300(6)	5.090(6)
		1.5	14.870(6)	6.010(6)
		2	16.490(5)	6.830(5)
		2.5	18.080(5)	7.910(5)
	308	0.25	11.870(6)	4.260(6)
		0.5	13.530(5)	5.110(5)
		1	15.080(5)	6.133(5)
		1.5	17.450(6)	7.173(6)
		2	19.070(6)	7.950(6)
		2.5	20.860(5)	8.930(5)

Table S6. Observed *pseudo*-first order rate constants as a function of ligand concentration and temperature for the substitution reactions between complex **2** and 5'-GMP in 25 mM Hepes buffer and 30 mM NaCl (pH=7.2).

λ/nm	T/K	$10^{-4}C_L$/M	k_{obs}/s^{-1}
255	288	0.25	0.488(5)
		0.5	1.010(6)
		1	1.580(5)
		1.5	1.980(6)
		2	2.572(5)
		2,5	3.143(5)
	298	0.25	0.810(6)
		0.5	1.403(5)
		1	2.010(5)
		1.5	2.585(6)
		2	3.158(5)
		2.5	3.628(5)
	308	0.25	1.205(6)
		0.5	1.906(6)
		1	2.680(6)
		1.5	3.230(5)
		2	3.988(5)
		2.5	4.650(5)

Table S7. Observed *pseudo*-first order rate constants as a function of ligand concentration and temperature for the substitution reactions between complex **2** and GSH in 25 mM Hepes buffer and 30 mM NaCl (pH=7.2).

λ/nm	T/K	$10^{-4}C_L$/M	k_{obs}/s^{-1}
294	288	0.25	0.835(5)
		0.5	1.274(5)
		1	1.867(6)
		1.5	2.410(5)
		2	3.020(5)
		2.5	3.586(5)
	298	0.25	1.100(5)
		0.5	1.620(5)
		1	2.170(5)
		1.5	2.910(6)
		2	3.370(5)
		2.5	4.090(6)
	308	0.25	1.270(5)
		0.5	2.020(5)
		1	2.690(6)
		1.5	3.420(5)
		2	4.240(5)
		2.5	4.830(6)

Table S8. Observed *pseudo*-first order rate constants as a function of ligand concentration and temperature for the substitution reactions between complex **2** and L-Met in 25 mM Hepes buffer and 30 mM NaCl (pH=7.2).

λ/nm	T/K	$10^{-4}C_L$/M	k_{obs}/s^{-1}
294	288	0.25	1.202(5)
		0.5	1.942(6)
		1	2.564(5)
		1.5	3.346(5)
		2	3.940(6)
		2.5	4.372(5)
	298	0.25	1.508(5)
		0.5	2.170(6)
		1	2.755(6)
		1.5	3.558(5)
		2	4.203(6)
		2.5	4.730(5)
	308	0.25	1.600(5)
		0.5	2.200(5)
		1	3.070(6)
		1.5	3.690(5)
		2	4.413(6)

Table S9. The effect of complexes **1** and **2** on MDA-231, HCT-116 and HaCaT cell lines viabilities, after 24 and 72 hours exposure. Results are expressed as absorbance.*$p<0.05$, treatment vs control.

Complex	Conc (μM)	MDA-MB-231		HCT-116		HaCaT	
		24h	72h	24h	72h	24h	72h
K (n=24)	0	0.89±0.03	2.10±0.16	0.79±0.11	1.54±0.24	1.25±0.25	2.22±0.38
1 (n=6)	0.1	1.01±0.05	1.94±0.32	0.62±0.09	0.90±0.34	1.30±0.18	2.30±0.20
	1	0.84±0.09	1.04±0.33	0.44±0.06	0.51±0.05	1.09±0.13	1.47±0.07
	10	0.75±0.03	0.86±0.23	0.36±0.03	0.22±0.02	0.64±0.09	0.22±0.05
	50	0.19±0.01	0.18±0.03	0.17±0.02	0.19±0.03	0.16±0.01	0.17±0.02
	100	0.19±0.02	0.17±0.02	0.18±0.03	0.19±0.03	0.16±0.01	0.18±0.01
	200	0.19±0.01	0.18±0.02	0.17±0.02	0.19±0.02	0.17±0.02	0.18±0.02
2 (n=6)	0.1	1.11±0.22	2.18±0.24	0.54±0.03	0.52±0.04	0.72±0.04	2.31±0.13
	1	1.11±0.06	1.19±0.25	0.49±0.05	0.24±0.03	0.99±0.06	1.41±0.08
	10	0.97±0.19	1.14±0.18	0.43±0.07	0.22±0.02	0.97±0.07	0.65±0.05
	50	0.65±0.08	0.79±0.14	0.27±0.03	0.19±0.03	0.95±0.03	0.34±0.03
	100	0.21±0.01	0.21±0.05	0.18±0.01	0.20±0.02	0.22±0.04	0.19±0.02
	200	0.17±0.02	0.18±0.02	0.17±0.02	0.20±0.02	0.17±0.01	0.19±0.01

Table S10. The effect of complexes **1** and **2** on MDA-231, HCT-116 and HaCaT cell lines viabilities, after 24 and 72 hours exposure. Results are expressed as percentages of viable cells in treatment compared to control/untreated cells (100%).

Complex	Conc (μM)	MDA-MB-231		HCT-116		HaCaT	
		24h	72h	24h	72h	24h	72h
1 (n=6)	0.1	114.32	92.33	78.36	58.28	103.82	103.59
	1	94.28	49.59	56.02	33.25	87.49	66.36
	10	84.17	40.96	45.40	14.20	50.76	9.79
	50	21.04	8.45	21.79	12.18	13.15	7.87
	100	21.02	8.26	22.81	12.56	13.04	8.32
	200	21.15	8.55	21.58	12.23	13.87	8.33
2 (n=6)	0.1	125.22	103.64	68.20	33.61	57.61	104.20
	1	124.90	56.65	62.05	15.78	79.88	63.54
	10	109.43	54.37	54.81	14.31	77.52	29.17
	50	73.86	37.38	34.69	12.32	75.67	15.48
	100	23.97	9.96	22.55	12.97	17.81	8.55
	200	19.72	8.36	21.75	12.70	13.32	8.62

Table S11. Coefficient of correlation (R) between concentrations of complexes **1** and **2** and cytotoxic effect on MDA-231, HCT-116 and HaCaT cell lines after 24 and 72 hours incubation. Results are calculated upon percentages of viable cells.*significant correlation (R≥0.70)

Au-complex	Coefficient of correlation (R)					
	MDA-MB-231		HCT-116		HaCaT	
	24h	72h	24h	72h	24h	72h
1	-0.77*	-0.69	-0.72*	-0.55	-0.73*	-0.57
2	-0.92*	-0.80*	-0.87*	-0.46	-0.86*	-0.67